

Advanced Computer Vision and Signal Processing for Quantitative Tremor and Gait Analysis in Parkinson's Disease: A Case Study

Authors and Affiliations:

Jack Bantley

Affiliation: U: The Mind Company, Charlotte, North Carolina, USA

Gowrish Rajagopal

Affiliation: U: The Mind Company, The Ohio State University, Columbus, Ohio, USA

Safwa Mohammed Abdul Jabbar

Affiliation: U: The Mind Company, Osmania University, Hyderabad, India

Divyam Sharma

Affiliation: Independent AI & Computer Vision Engineer, India

Mihirsinh Chauhan

Affiliation: U: The Mind Company, Sardar Vallabhbhai National Institute of Technology, Surat, India

Mohammed (Mo) Abouelsoud

Affiliation: U: The Mind Company, Cleveland, Ohio, USA

Shwetan Varanasi

Affiliation: U: The Mind Company, The Ohio State University, Columbus, Ohio, USA

David Michelevich MD PhD

Affiliation: U: The Mind Company, Playa Del Rey, California, Ohio, USA

Abstract

Tremor analysis plays a vital role in understanding motor control disorders and enhancing diagnostic accuracy for conditions like Parkinson's disease (PD), essential tremor, and related neurodegenerative disorders. In this study, we present a comprehensive approach to analyzing tremor and gait dysfunction across the entire body using advanced computer vision (MMPose) and signal processing methodologies. By extracting time-domain features, applying spectral analysis, and examining temporal dynamics of tremor symptoms, we aim to provide detailed quantitative insights into both motor and gait patterns. Additionally, we

illustrate the clinical relevance of our methods through a case study of a 63-year-old male diagnosed with PD, treated with repeated sessions of transcranial electrical stimulation. The patient's therapy outcomes, characterized by extended tremor relief lasting up to seven hours and notable improvements in rigidity, underscore the utility of our multi-faceted analytical framework. Overall, these findings highlight the value of integrating computer vision and signal processing for more precise diagnosis and management of tremor-related conditions.

Keywords

Tremor Analysis, Signal Processing, Time-Domain Features, Spectral Analysis, Motor Disorders, Computer Vision

1. Introduction

Tremors are involuntary, rhythmic oscillations or movements of body parts that can affect various regions of the body, including the upper extremities (hands, arms, fingers), lower extremities (legs, feet), trunk, and head/neck region. They are one of the most common types of abnormal movements observed in neurological disorders, and they can significantly impact an individual's quality of life (Hallett, 2011). While tremors themselves are not a disease, they can be indicative of underlying neurological conditions, such as Parkinson's disease (PD), essential tremor (ET), or other neurological disorders (Deuschl et al., 1998). Understanding tremors, their causes, and their frequencies is critical for diagnosing and managing these conditions, especially given their prevalence in aging populations (Elble, 2013).

Tremors in Parkinson's Disease

Parkinson's disease (PD) is a progressive neurodegenerative disorder primarily affecting motor function. While the characteristic resting tremor typically begins in the hands, manifesting as a "pill-rolling" motion between the thumb and forefinger, PD tremors can affect multiple body regions as the disease progresses (Zach et al., 2015). These tremors may involve the legs, jaw, tongue, and trunk, creating a more generalized tremor pattern. The tremors occur at frequencies between 4-6 Hz, although they can vary among individuals. They are most pronounced during rest and often diminish with voluntary movement (Louis, 2005).

The widespread nature of PD tremors reflects the extensive involvement of the brain's motor pathways, primarily due to the degeneration of dopaminergic neurons in the substantia nigra (Hallett, 2012). This degeneration can lead to both unilateral and bilateral tremors, though asymmetry is common, particularly in early stages. Additionally, it's important to note the existence of drug-induced parkinsonism, where medications such as antipsychotics, antiemetics, or certain calcium channel blockers can induce or exacerbate parkinsonian tremors (O'Suilleabhain & Matsumoto, 1998). Conversely, some medications used to treat PD, particularly dopamine agonists, may paradoxically worsen tremors in some patients, highlighting the complex relationship between pharmacological interventions and tremor manifestation (Gerald & Evidente, 2023).

Parkinson's disease tremors are not only a source of physical discomfort but also a significant cause of disability. They can affect an individual's ability to perform basic activities such as writing, eating, and dressing, leading to a decrease in independence and quality of life (Baumann, 2011). Treatment options often involve medications such as levodopa, and deep brain stimulation (DBS) remains a well-established surgical intervention, while newer non-invasive approaches like transcranial electrical stimulation (tES) show promising results (Deuschl et al., 1998). tES techniques can modulate neural activity in targeted brain regions, potentially helping to manage tremor symptoms across various neurological conditions. The non-invasive nature of tES makes it an attractive option for patients who may not be candidates for surgical interventions or prefer less invasive treatments (Hallett, 2011).

Tremors in Essential Tremor

Essential tremor (ET) is another prevalent neurological disorder characterized by rhythmic shaking, usually in the hands, but it can also affect the head, voice, and sometimes the legs (Louis, 2005). Unlike Parkinson's disease, ET is not associated with other significant neurological impairments, and it is often familial, meaning it can run in families (Elble, 2013). ET tremors are typically action-induced, occurring during voluntary movement rather than at rest, making it distinct from the resting tremors seen in Parkinson's disease (Gerald & Evidente, 2023). The tremors in essential tremor typically occur at 6-12 Hz and are usually more noticeable when performing tasks that require fine motor control, such as writing, drinking from a glass, or using utensils (Baumann, 2011).

While essential tremor is considered less disabling than Parkinson's disease, it can still have a profound impact on an individual's functional ability and emotional well-being. In severe cases, it can interfere with daily activities and lead to social embarrassment (Hallett, 2011). The pathophysiology of essential tremor remains less understood, but it is thought to involve abnormal brain activity in the cerebellum, the part of the brain responsible for coordinating movement (Deuschl et al., 1998). Management of ET includes medications like beta-blockers (e.g., propranolol) or anticonvulsants (e.g., primidone), and in some cases, surgical interventions such as deep brain stimulation (DBS) and transcranial electrical stimulation (tES) techniques (Zach et al., 2015).

Tremors in Other Neurological Disorders

Beyond PD and ET, tremors are prevalent in various other neurological conditions, each with distinct characteristics and mechanisms. Multiple sclerosis (MS) can produce intention tremors due to cerebellar involvement, typically presenting during goal-directed movements (Hallett, 2012). Post-stroke tremors may develop as a consequence of cerebellar or thalamic lesions, often manifesting as intention or postural tremors (O'Suilleabhain & Matsumoto, 1998). Psychological tremors, also known as psychogenic tremors, can occur in anxiety disorders or conversion disorder, typically presenting with variable frequency and amplitude, and often increasing with attention (Gerald & Evidente, 2023). These tremors may be accompanied by other psychological symptoms and typically show entrainment with voluntary movements (Louis, 2005).

The Role of Tremor Frequency

The frequency of tremors plays a critical role in differentiating between various types of tremor disorders. While tremors associated with Parkinson's disease typically occur in the 4-6 Hz range, those associated with essential tremor typically present at higher frequencies, usually in the 6-12 Hz range (Zach et al., 2015). These frequency patterns can aid in the clinical differentiation between Parkinson's disease and essential tremor, although overlap can occur in some cases (Baumann, 2011). Tremor frequency is often measured using techniques like electromyography (EMG) or accelerometry, which can provide valuable diagnostic information and guide therapeutic decisions (Elble, 2013).

Understanding the frequency of tremors, along with their other characteristics, is crucial for proper diagnosis and treatment planning. Tremor frequency not only serves as a distinguishing feature between conditions like Parkinson's disease and essential tremor but also helps track the progression of these disorders and evaluate the effectiveness of treatment options (Deuschl et al., 1998).

This paper presents an automated approach to analyze tremor data, focusing on extracting temporal and spectral features from video-recorded movements processed into numerical datasets, considering the full range of tremor manifestations across different body regions and neurological conditions (Hallett, 2011).

Case Study Overview

To demonstrate the practical impact of our methodological approach, we incorporate a case study of a 63-year-old male patient diagnosed with Parkinson's disease in January 2024. His primary complaints included a right-hand tremor and pronounced rigidity in the shoulders, hips, hands, and lower back. Throughout a series of non-invasive transcranial electrical stimulation treatments, administered at electrode positions (C3, C4, F7, F8) and gradually increased from 4 mA to 8 mA, he recorded daily observations of tremor relief, typically ranging from one to seven hours depending on treatment schedule and medication adherence. Videos captured pre- and post-treatment were processed through the MMpose system to extract key metrics such as tremor amplitude, PSD in the 3–12 Hz range, and various gait parameters including step length and timing. These quantitative measures corroborated the patient's reports of fluctuating yet ultimately improving tremor control and reduced rigidity, underscoring how integrated analytics can illuminate both short-term effects and the challenges of sustaining symptom relief amid real-world constraints.

2. Methodology

Data Acquisition

The data for this study was collected using MMpose, an open-source computer vision-based toolkit from OpenMMLab that specializes in pose estimation and tracking. MMpose provides comprehensive whole-body analysis capabilities, detecting and tracking key points across the

entire human body including hands, face, body, and feet. The system employs deep learning models, specifically convolutional neural networks (CNNs), to simultaneously track multiple keypoints across different body parts with high precision.

For hand tremor analysis, MMPOse tracked hand movements from video recordings of patients experiencing tremors. The software processes each video frame through its neural network architecture to detect keypoints on the hands, with particular focus on anatomical landmarks such as finger joints and wrist positions. MMPOse's modular design allows for real-time tracking while maintaining high accuracy in keypoint detection even under varying lighting conditions and hand orientations. These keypoints were used to calculate Euclidean distances between consecutive positions across frames, serving as indicators of tremor amplitudes. The resulting data was stored in a CSV file, with each row corresponding to a frame in the video and containing the Euclidean distances between the keypoints.

For gait analysis portion of the study, MMPOse tracked the entire wireframe of the human along with their movements from recordings of a patient walking back and forth across a relatively flat surface. MMPOse employs deep learning to estimate the key points of 2D images. The software processed each frame of the video to detect keypoints for the entire body, ranging from the face to the heel, and provided fairly precise body part positions over time. The recorded keypoints, which were at significantly anatomical landmarks, were used to calculate Euclidean distances between consecutive keypoints across frames. These distances served as an indicator of tremor amplitudes, providing valuable information about the severity and frequency of tremors. The resulting data was stored in a CSV file, with each row corresponding to a frame in the video and containing the Euclidean distances between the keypoints. Another CSV file was created to store the keypoints of the various positioning of the joints found by the MMPOse software for future use. **Figure 1** provides an overview of the data processing workflow used in this study, highlighting the key steps from loading raw tremor data to generating frequency and spectral analyses. The diagram demonstrates the systematic approach taken to handle missing values, apply preprocessing techniques, and extract meaningful features for tremor analysis, ensuring a robust and accurate analysis pipeline.

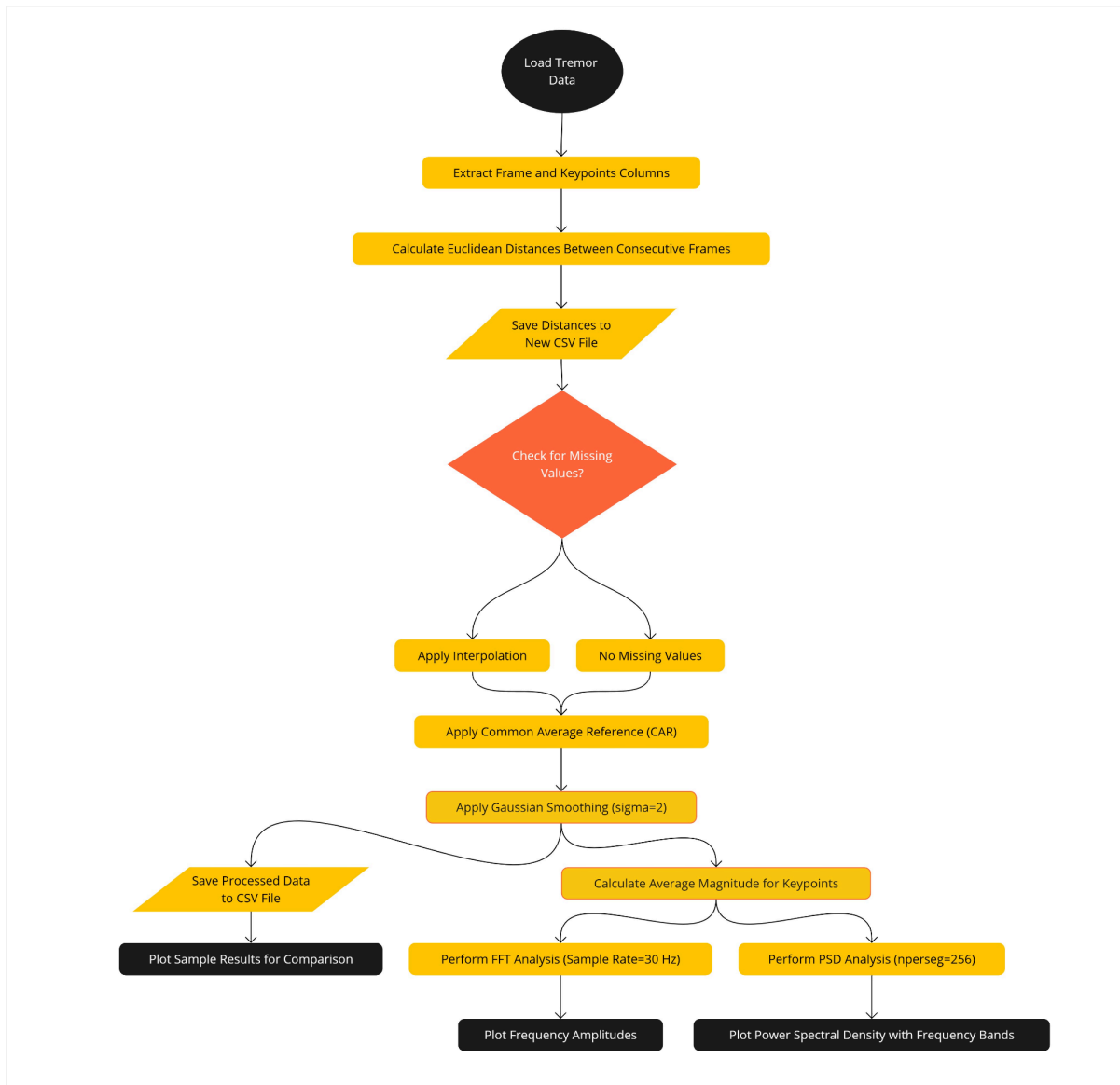


Figure 1.

Data Cleaning

The raw data obtained from the video recordings was subject to a series of pre-processing steps to ensure its reliability for subsequent analysis. One of the initial steps was the application of the **Common Average Referencing (CAR)** technique. This method aimed to correct for common disturbances or artefacts in the data that could affect the accuracy of tremor measurements. By using CAR, we were able to remove common noise sources and ensure that the data more accurately reflected the true tremor activity of the patient.

Common Average Referencing (CAR)

The Common Average Referencing (CAR) method is used to reduce common noise across multiple signals by referencing each signal to the average of all signals. For a dataset containing N signals the CAR-transformed signal S'_i for the i-th signal is computed as:

$$S'_i(t) = S_i(t) - \frac{1}{N} \sum_{j=1}^N S_j(t)$$

Where:

- $S_i(t)$ is the original signal at time t for the i-th channel.
- $S'_i(t)$ is the CAR-transformed signal at time t for the i-th channel.
- N is the total number of signals (or channels).
- $\frac{1}{N} \sum_{j=1}^N S_j(t)$ represents the average of all signals at time t.

Explanation:

Original Signal $S_i(t)$: This is the raw data recorded at a specific channel or electrode.

Average Signal: At each time point t, the average of all signals across the N channels is calculated. This average captures the common noise or baseline activity shared across all channels.

Explanation:

Original Signal $S_i(t)$: This is the raw data recorded at a specific channel or electrode.

Average Signal: At each time point t, the average of all signals across the N channels is calculated. This average captures the common noise or baseline activity shared across all channels.

Subtraction: By subtracting the average signal from the original signal, the CAR method effectively reduces shared noise or artifacts, enhancing the relative differences between channels.

This method aimed to correct for common disturbances or artefacts in the data that could affect the accuracy of tremor measurements. By using CAR, we were able to remove

common noise sources and ensure that the data more accurately reflected the true tremor activity of the patient.

Further refinement of the data was done using a **Gaussian filter**, which was applied to smooth the Euclidean distance data. The Gaussian filter is a low-pass filter that reduces high-frequency noise, which is particularly important for tremor data that may exhibit fluctuations due to minor variations in the video recording or environmental factors. This process helped improve the signal-to-noise ratio, ensuring that only relevant tremor activity was retained for analysis.

The Gaussian filter is based on the Gaussian function:

$$G(x) = (1/\sqrt{2\pi\sigma^2})e^{(-x^2/2\sigma^2)}$$

Where:

- $G(x)$ is the Gaussian function value at x .
- σ is the standard deviation, which determines the width of the Gaussian kernel and controls the degree of smoothing.

Applying the Gaussian Filter

To smooth a time-series signal or spatial data:

1. A **Gaussian kernel** is created using the Gaussian function, centered at zero, with a size that typically spans $\pm 2\sigma$.
2. The signal $S(t)$ is convolved with the Gaussian kernel $G(x)$ as:

$$S'(t) = \sum_{x=-k}^k S(t + x) \cdot G(x)$$

Where:

- $S'(t)$ is the smoothed signal at time t .
- $S(t + x)$ represents the signal values in a window around t .
- $G(x)$ is the Gaussian kernel value corresponding to offset x .
- k is the kernel half-width, often 3σ .

Key Features:

- **Weighted Averaging:** The Gaussian filter performs weighted averaging, where values closer to the center have higher weights, reducing the impact of distant noise.
- **Smoothing:** High-frequency noise, such as rapid fluctuations, is diminished, leaving smoother and more relevant tremor data.

Feature Analysis

Once the data was cleaned and pre-processed, several key features were extracted to characterize the tremor activity. These features are crucial for quantifying tremor severity and understanding its underlying dynamics.

1. **Amplitude Calculation:** **Amplitude Calculation:** To quantify the severity of the tremor, the **absolute amplitude** of hand movements was calculated for each frame. The amplitude is defined as the Euclidean distance between keypoints, representing the magnitude of the tremor. This measure allows for an evaluation of how much the tremor displaces the hand over time. A higher amplitude generally corresponds to more severe tremors, which can be used to assess the progression of the disorder or the effectiveness of treatment interventions.
2. **Power Spectral Density (PSD):** To analyze the frequency characteristics of the tremors, a **Power Spectral Density (PSD)** analysis was performed. The PSD provides a visualization of how the power of the tremor signal is distributed across various frequency components. For tremors, we focused on the **3-12 Hz frequency band**, which is typically associated with tremor activity, with the most relevant frequencies often falling in the lower range of this band. By performing a Fourier transform on the data, we could evaluate the spectral components of the tremor and identify any frequency shifts or changes over time. This frequency-based analysis is crucial for understanding the nature of the tremor, as different tremor types (e.g., Parkinsonian vs. essential tremor) have distinct frequency characteristics.
3. **Step Timing Calculation:** For calculating the timings taken for the subject to take a step, the key positions of the patient's heels were analyzed. Initially, the data

underwent a Gaussian filter to smooth out noise and irregularities. The Gaussian filter is based on the Gaussian function:

$$G(x) = (1/\sqrt{2\pi\sigma^2})e^{(-x^2/2\sigma^2)}$$

Where:

- $G(x)$: Gaussian function value at x .
- σ : Standard deviation, determining the width of the kernel and the degree of smoothing.

Following this, a dynamic threshold was determined based on a rolling window of the last 10 frames of the data. This threshold was calculated using the mean (μ) and standard deviation σ of heel movement within the window:

$$\text{Threshold} = \mu_{\text{heel}} + k \cdot \sigma_{\text{heel}}$$

Where k is a scaling factor.

It served to identify whether the heel was stationary, marking a foot strike on the ground. The duration of each step was then calculated by measuring the time between the strike of one heel and the subsequent strike of the opposite heel. The program evaluated all heel position inputs from both legs to calculate the number of frames that elapsed between alternating heel strikes. These frame counts were converted into time durations using the frame rate of the data.

$$\text{Time Duration} = \text{Frame Count} / \text{Frame Rate}$$

If the calculated step time exceeded a minimally viable threshold (set to 0.5 seconds in this instance), it was recorded in 1-D series. This series stores all step times and will later be used to plot and analyze the patient's gait patterns.

4. **Swing Timing Calculation:** For calculating the timings taken for the subject to take a swing, the calculations had to be broken down to each left and right leg. The Gaussian filtering was also applied to the dataset. A dynamic threshold was also implemented

in the same manner as the step timing, where the mean and standard deviation of heel movement from the rolling window of the last 10 frames for the data were used.

Eventually, the program categorizes the movements as each leg takes a full swing through measuring the time between the strike of one heel and the subsequent strike of the same heel once again. The code helps to find the number of frames that had elapsed between the heel strikes. The frame count is then converted into time duration using the frame rate of the data. If the calculated step time exceeded a minimally viable threshold (set to 0.7 seconds for this), it was recorded in two 1-D series that stored the durations for each foot separately. These series store all stride times and will later be used to plot and analyze the patient's gait patterns.

5. **Step Length Calculation:** For calculating the step length, the displacement of the patient's heel position for each step was analyzed. A Gaussian filter was applied to the data to smooth out noise and irregularities in the positional data. Following this, a dynamic threshold was implemented using the rolling window of the last 10 frames, with the mean and standard deviation of the heel positions used to identify significant movements indicative of a step. The program later identified the heel strikes for each leg by evaluating when the vertical position of the heel fell below and rose above the threshold. For each pair of alternating heel strikes from each leg (left-right or right-left), the Euclidean distance between the respective heel positions was calculated in pixel units.

$$\text{Euclidean Distance} = \sqrt{(x_2 - x_1)^2 + (y_2 - y_1)^2}$$

Using the real world measurement from the subject's known physical height, the pixel-length measurement was scaled to a real-world measurement. Results were further filtered with the lengths exceeding a minimally viable threshold being included in a 1-D series for further analysis. The step length measurement will be used to provide more details about the subject's walking patterns.

6. **Stride Length Calculation:** To calculate the stride length, the displacement of the patient's heel position was used. A Gaussian filter was applied to the data for smoothing out noise and irregularities. Following this, a dynamic threshold was implemented using the rolling window of the last 20 frames, with the mean and standard deviation of the heel positions used to identify significant movements

indicative of a step. The program later identified the heel strikes for each leg by evaluating when the vertical position of the heel fell below and rose above the threshold. Consecutive heel strikes from the same leg (left-left or right-right) were used to measure the Euclidean distances between the heel positions in pixel units.

$$\text{Euclidean Distance} = \sqrt{(x_2 - x_1)^2 + (y_2 - y_1)^2}$$

Using the real world measurement from the subject's known physical height, the pixel-length measurement was scaled to a real-world measurement. Results were further filtered with the lengths exceeding a minimally viable threshold being included in a 1-D series for further analysis. The stride length measurement will be used to provide more details about the subject's walking patterns.

7. **Additional Metrics Calculation:** Several other metrics were calculated to provide a comprehensive view of the tremor characteristics. These included:
 - o **Absolute Average Amplitude:** The average magnitude of the tremor over time, providing an overall sense of tremor severity.
 - o **Peak Amplitude:** The maximum displacement of keypoints within a given time window, which helps in identifying the most intense tremor episodes

Visualization

The final step in the analysis involved visualizing the cleaned and processed data to better understand the temporal and spectral characteristics of the tremor. Several types of visualizations were created:

- **Time-domain Plots:** These plots show the tremor amplitude over time, highlighting periods of increased tremor intensity. Time-domain analysis provides a clear picture of how the tremor evolves and can reveal patterns, such as the presence of rhythmic oscillations that are indicative of specific tremor types (e.g., essential tremor or Parkinsonian tremor).
- **Power Spectral Density (PSD) Plots:** The PSD plots were used to assess the distribution of power across various frequency bands, focusing on the 3-12 Hz range associated with tremor activity. These plots allowed for the identification of dominant frequencies in the tremor signal and enabled the classification of tremor types based on their spectral characteristics.

3. Case Summary

Patient Information

- **Age:** 63
- **Diagnosis date:** January 2024
- **Initial symptoms:** Right hand tremor, rigidity in shoulders, hips, hands, lower back
- **Medication:** Levodopa (37.5 mg, 4x daily)

Methods

- **Treatment device:** Sphere
- **Electrode placement:** C3, C4, F7, F8
- **Initial parameters:** 4 mA, later increased to 8 mA
- **Treatment duration:** 15 minutes per session
- **Treatment period:** September 9 to October 24, 2024

Results

Tremor Relief Progression

- **Initial:** 1-1.5 hours post-treatment
- **Improved to:** Up to 7 hours post-treatment

Rigidity Assessment

- **Initial:** 8/10
- **Final:** 3/10

In summary, the subject is a 63-year-old male diagnosed with Parkinson's in Jan of 2024. He became suspicious of Parkinson's while eating dinner because he could not physically get food from his plate into his mouth. His arm and hands simply froze 2-3 inches from his mouth. His primary symptoms are right-hand tremor and overall rigidity, with an emphasis on his shoulders, hips, hands, and lower back. The subject stated that his tremors cause him no pain. His biggest concern, relative to quality of life, is rigidity.

Once diagnosed, he was prescribed Levodopa 4 times per day, 37.5 mg per dose. He has struggled with intestinal issues and often skips doses because he cannot eat with an upset stomach.

Treatment Details

Consented treatments began with Sphere on Sept 9th for 15 minutes with electrodes positioned at C3 + C4 and F7 + F8 at 4 mA. Ultrasound gel was placed on each electrode. The subject stated there was slight discomfort when initially placing the electrodes from the pins, but that discomfort faded away in a couple of minutes. He also said he felt no electrical sensation at all. He did experience phosphenes if he closed his eyes. In his pre-treatment videos, there is an obvious resting tremor in both hands. In his gait video, he is very upright with very little arm swing, and short steps. There were multiple breaks in the treatments due to his travel schedule, and we did not treat on weekends.

After 5 days of treatment, the subject was very happy to report his overall rigidity had greatly improved. His arms were swinging and stride improved in length and cadence. He plays golf and reported, "today I could make a shoulder turn." In addition, post-treatment each day we saw full tremor relief beginning for about 1 to 1 1/2 hours and progressing to 4 1/2 to 5 hours, i.e., his tremors functionally did not interfere with daily activities, e.g., navigating the computer mouse or typing.

Observations and Outcomes

- **Day 8, 9/18/24:** Last treatment before his first out-of-town trip. On 9/23/24, he reported active tremors, but his upper body and gait felt good. By 9/26/24, he reported that gait was okay, but shoulders and upper body were getting stiff again. Treatments resumed on 9/30/24 after a 12-day break, with post-treatment relief of 4 ½ hours.
- **10/14/24:** Amperage was increased to 8mA. The subject still reported no electrical sensation but experienced phosphenes when closing his eyes. After 12 days without treatment, the device no longer had an impact on his symptoms. Upon resuming treatment, he reported 4 hours of tremor relief and noted a reduction in rigidity from 8 to 4 on a 10-point scale.
- **10/24/24:** On the last day of treatment, the subject reported tremor relief lasting 7 hours, with rigidity reduced to 3. He stated that the device provided freedom in all joints, shoulders, hands, hips, and lower back.

Conclusion

The subject is very happy with the impact Sphere has on his rigidity, his primary concern, and while we saw progressive improvement in the right-hand tremor in terms of length of post-treatment relief, up to 7 hours, he is not convinced the technology is effective with that symptom. The subject is grateful to have had an opportunity to participate in this study and looks forward to our development and optimization of the device.

RESULTS

Quantitative Tremor Analysis

Methodology

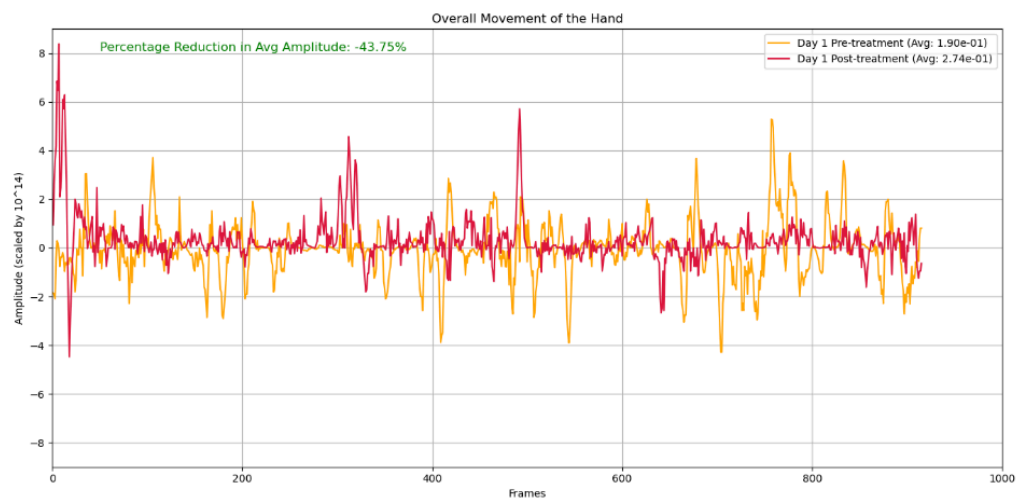
Hand tremor was objectively assessed using computer vision techniques applied to pre- and post-treatment video recordings. The analysis focused on multiple metrics:

- Data cleaning using noise reduction techniques
- Amplitude calculations
- Power Spectral Density (PSD) analysis in the 3-12 Hz tremor-associated frequency band

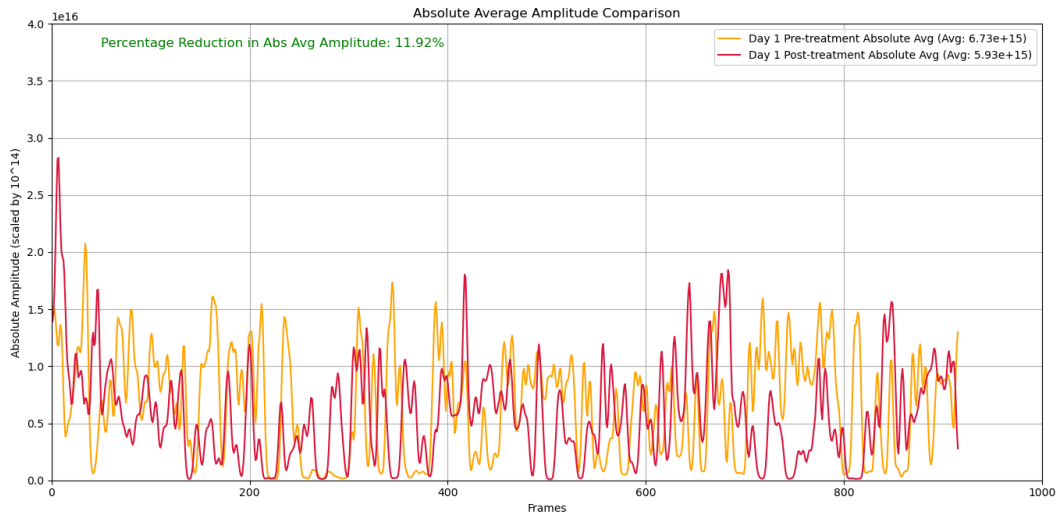
Tremor Progression Analysis

Day 1

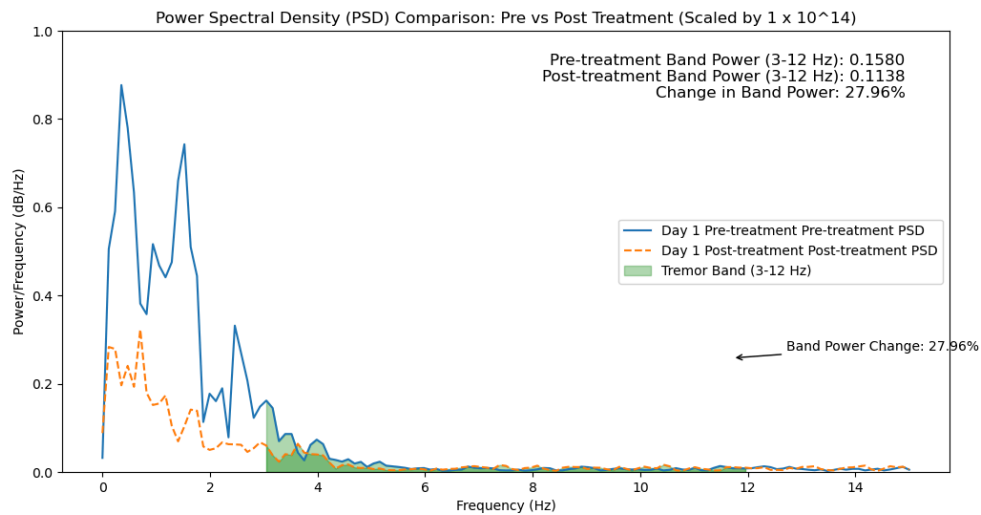
- **Figure 2: Overall Movement of the Hand:** The plot shows a **43.75% reduction** in overall hand movement, reflecting improved hand stability after treatment.



- **Figure 3: Absolute Average Amplitude Comparison:** This figure shows the absolute average amplitude before and after treatment on Day 1. The reduction of **11.92%** indicates a decrease in tremor severity.



- **Figure 4: Power Spectral Density (PSD) Comparison:** The PSD plot highlights a **27.96% reduction** in the 3-12 Hz frequency band, showing effective reduction in oscillatory activity.



Day 3

- **Figure 5: Overall Movement of the Hand:** A **33.33% reduction** in average amplitude is observed, indicating continued improvement in reducing hand movement.

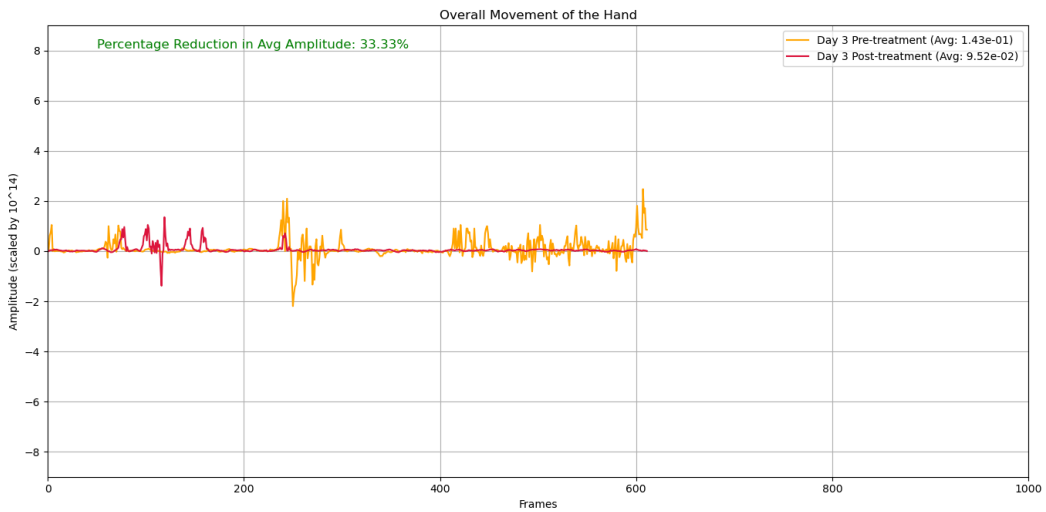


Figure 6: Absolute Average Amplitude Comparison: Day 3 shows an impressive **84.03%** reduction in average amplitude, suggesting significant treatment efficacy

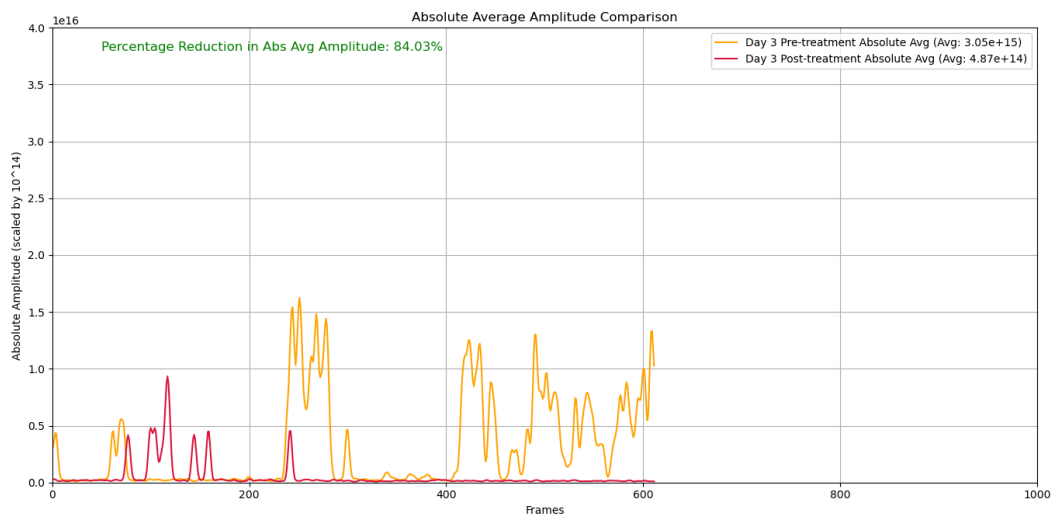
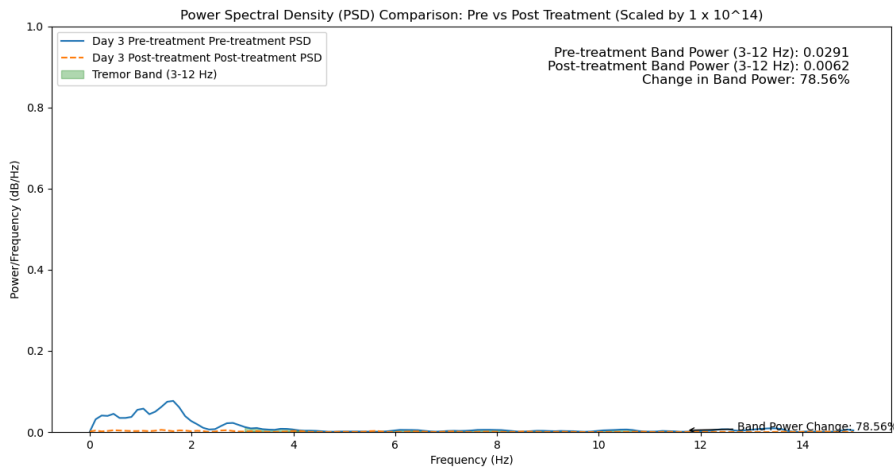
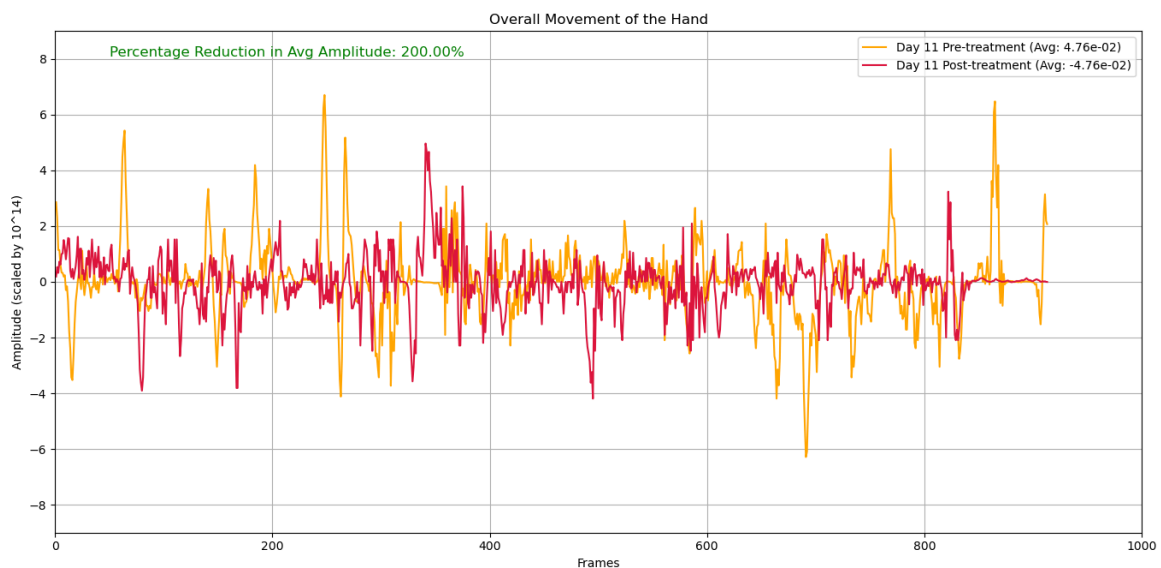


Figure 7: Power Spectral Density (PSD) Comparison: The **78.56% reduction** in the tremor band power (3-12 Hz) indicates a substantial decrease in tremor activity.

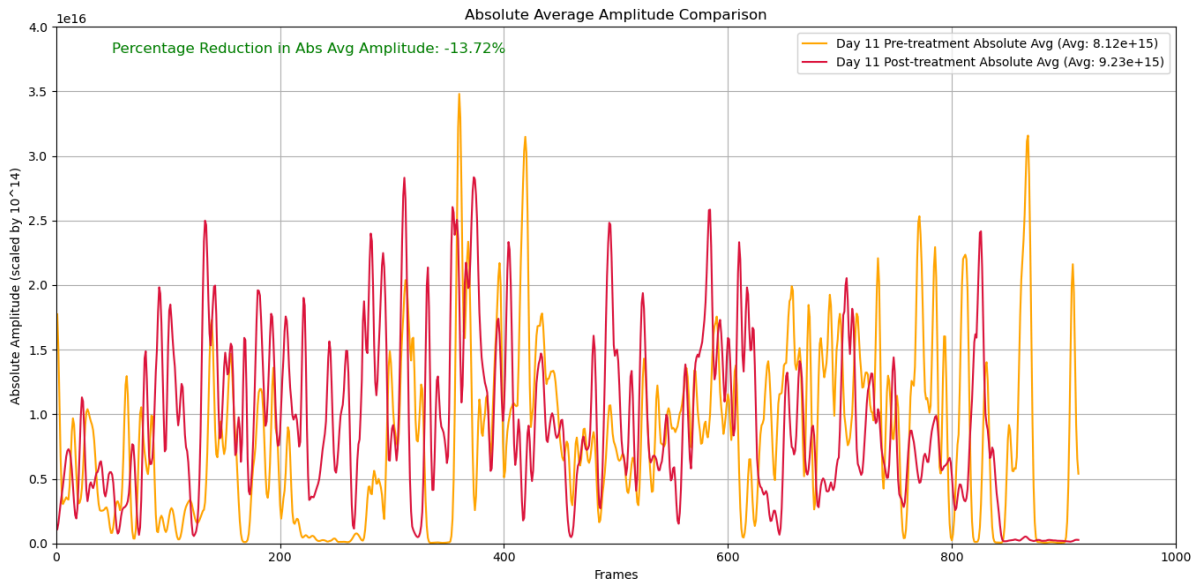


Day 11

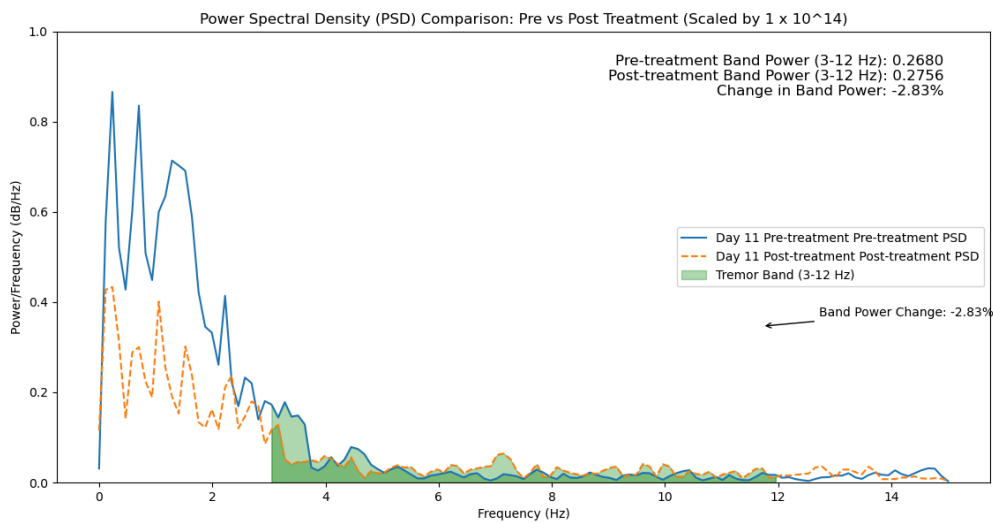
- **Figure 8: Overall Movement of the Hand:** The **-200% change** reflects increased instability in hand movement, implying the treatment was not effective on this day.



- **Figure 9: Absolute Average Amplitude Comparison:** On Day 11, there was a **-13.72% increase** in amplitude, suggesting decreased treatment effectiveness on this day.

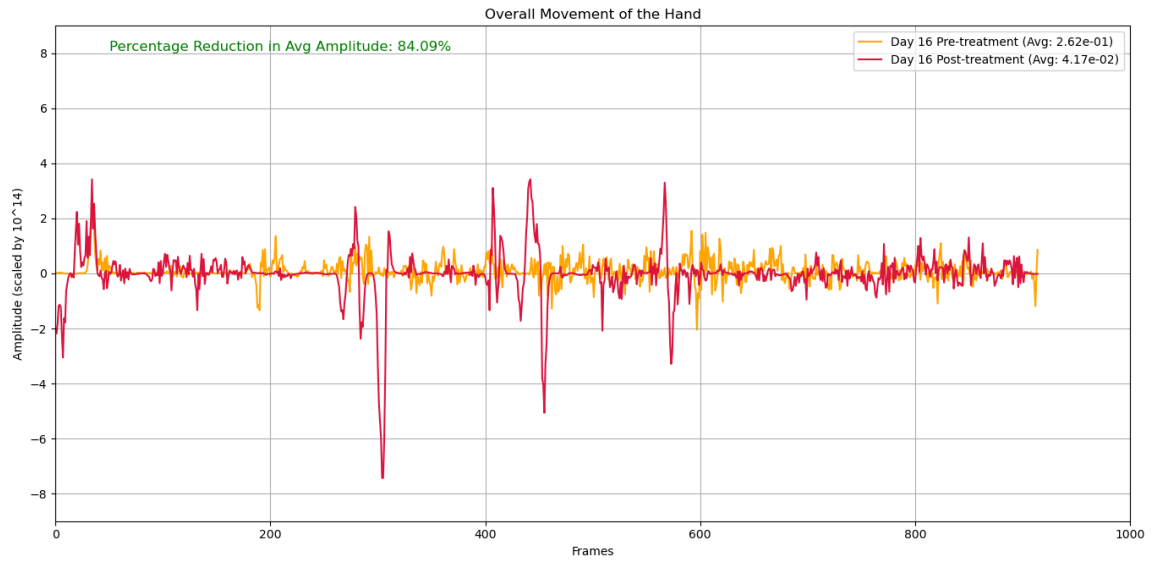


- **Figure 10: Power Spectral Density (PSD) Comparison:** The PSD plot shows a **2.83% increase** in the 3-12 Hz band power, indicating an increase in tremor activity.

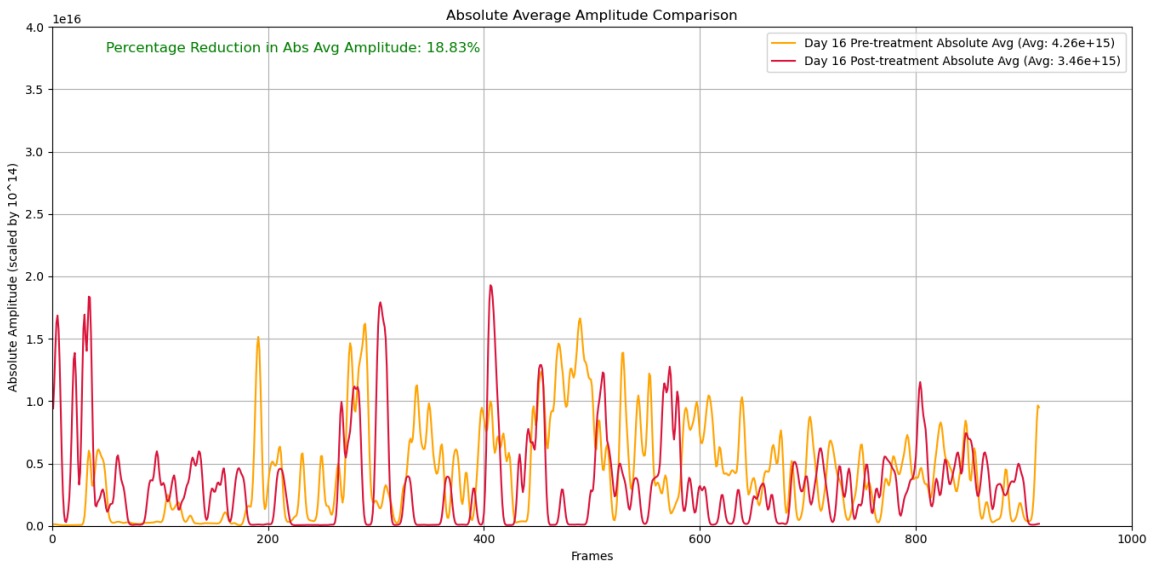


Day 16

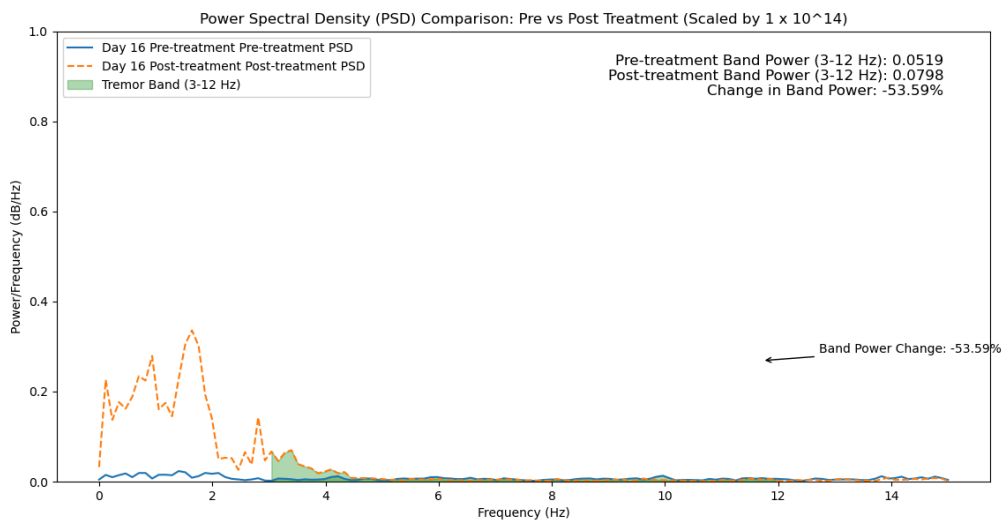
- **Figure 11: Overall Movement of the Hand:** The plot shows an **84.09% reduction** in average amplitude, indicating notable improvement in stability.



- **Figure 12: Absolute Average Amplitude Comparison:** There was an **18.83% reduction** in average amplitude, showing moderate effectiveness.

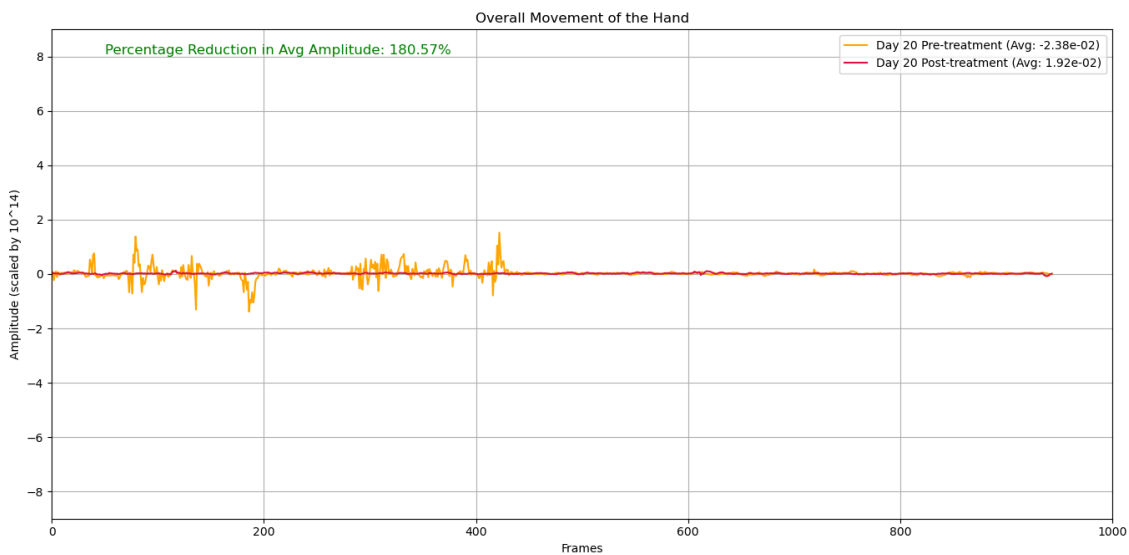


- **Figure 13: Power Spectral Density (PSD) Comparison:** The PSD analysis indicates a **-53.59% change** in tremor power, suggesting increased activity in the 3-12 Hz range post-treatment.

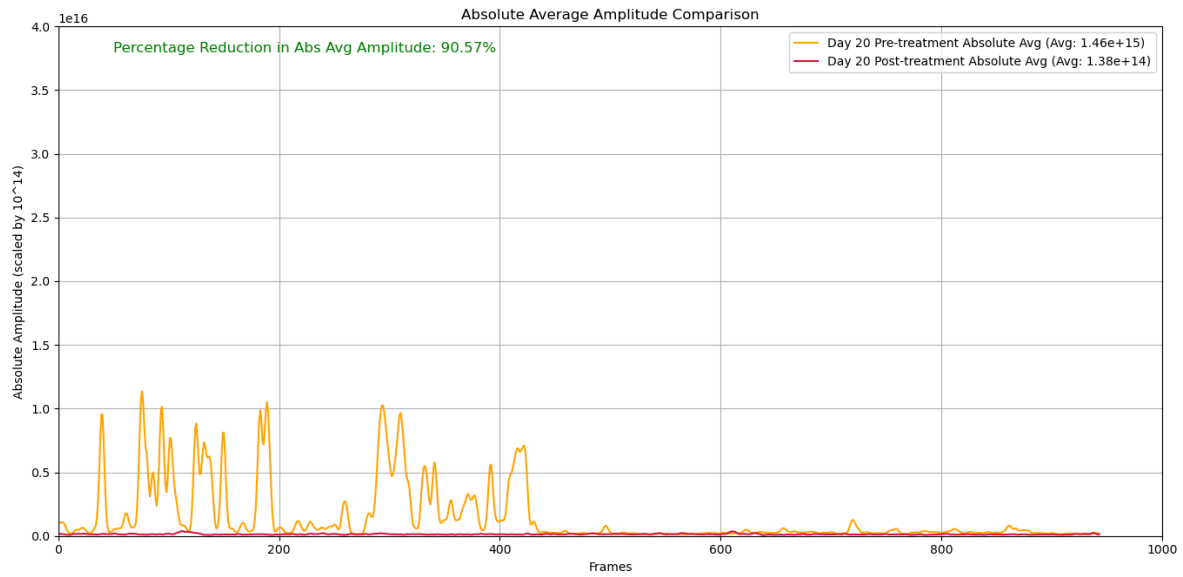


Day 20

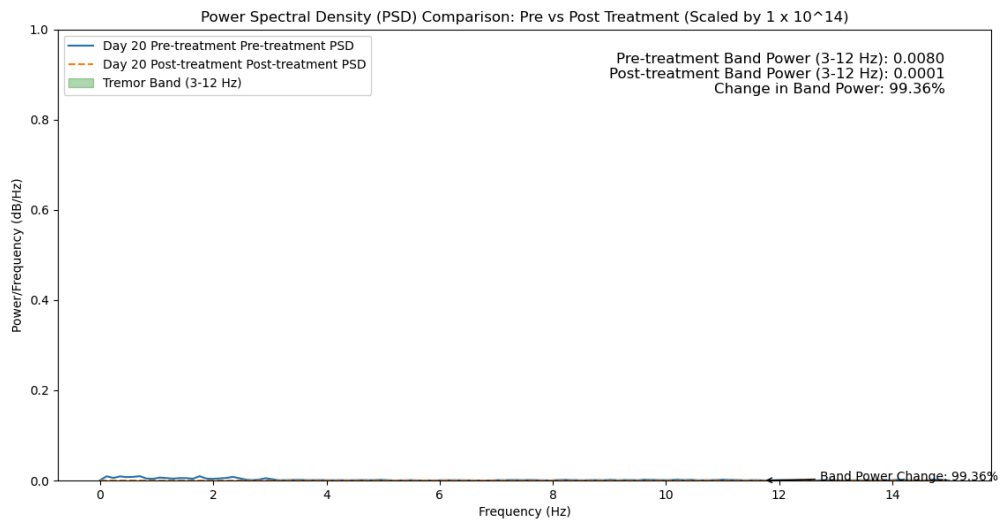
- **Figure 14: Overall Movement of the Hand:** The figure shows a **180.57% reduction** in average amplitude, demonstrating substantial improvement in stability.



- **Figure 15: Absolute Average Amplitude Comparison:** A **90.57% reduction** in absolute average amplitude suggests a strong reduction in tremor.



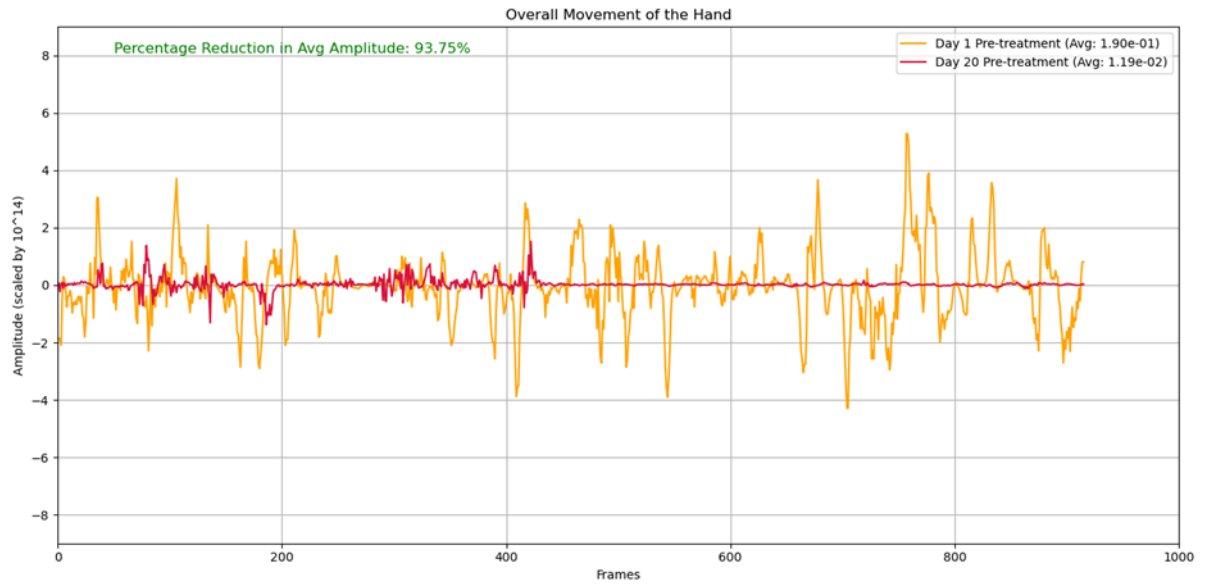
- **Figure 16: Power Spectral Density (PSD) Comparison:** The 99.36% reduction in tremor power further supports the effectiveness of the treatment on Day 20.



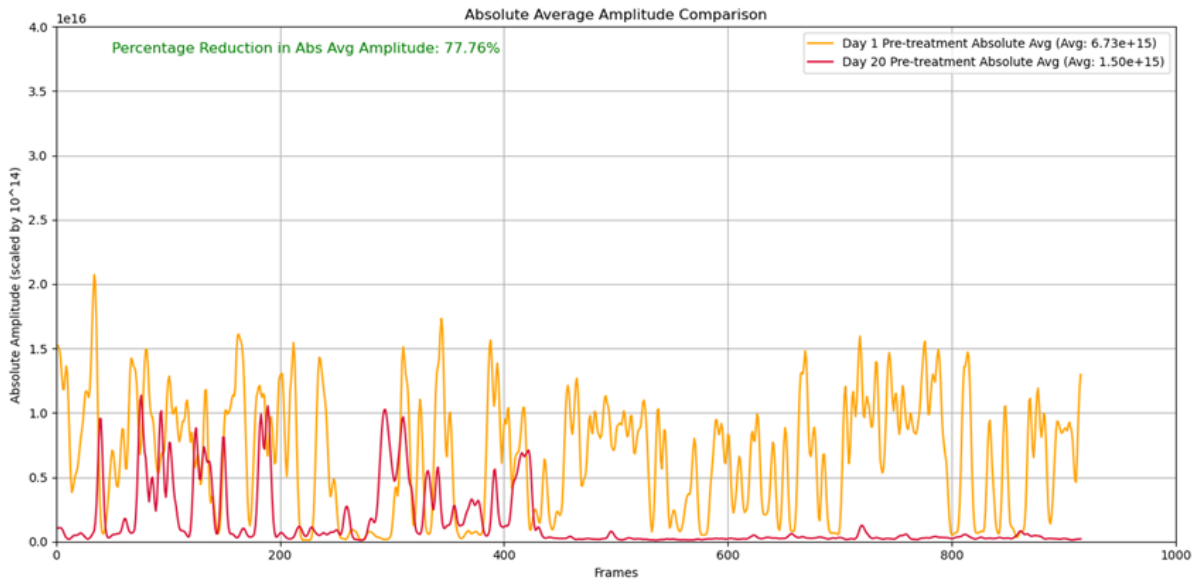
Day 1 vs Day 20 Pre-treatment Comparison

Side by side comparisons of Day 1 and Day 20 Pre-treatment results.

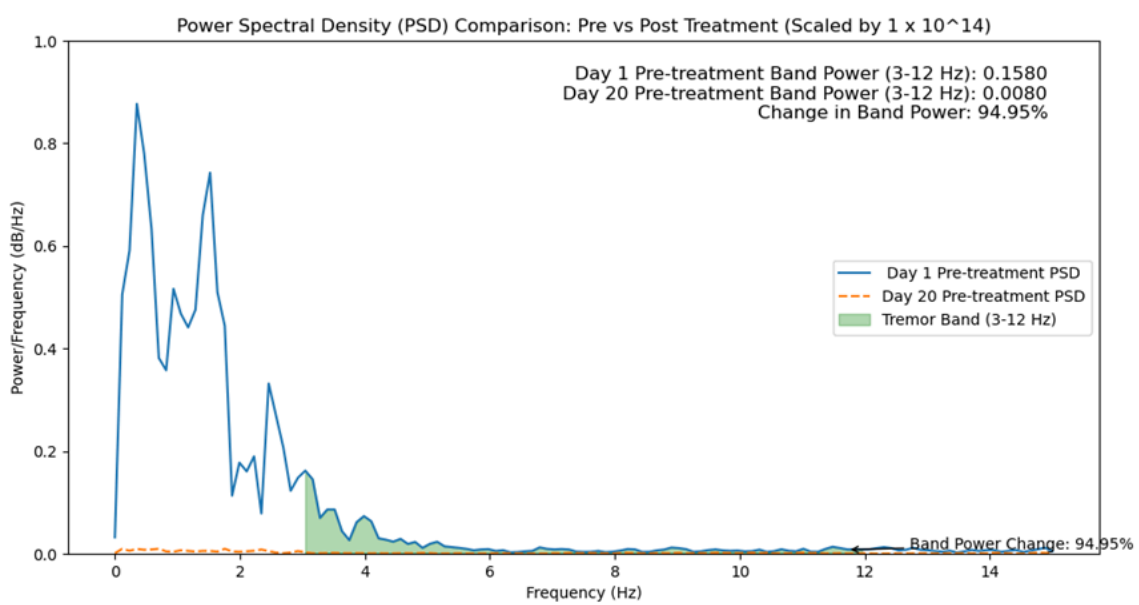
- **Figure 17: Overall Movement of the Hand:** The plot shows a 93.75% reduction in overall hand movement, reflecting significant improve hand stability on first and last day pre-treatment.



- **Figure 18: Absolute Average Amplitude Comparison:** A 77.76% reduction in absolute average amplitude suggests a strong reduction in tremor.



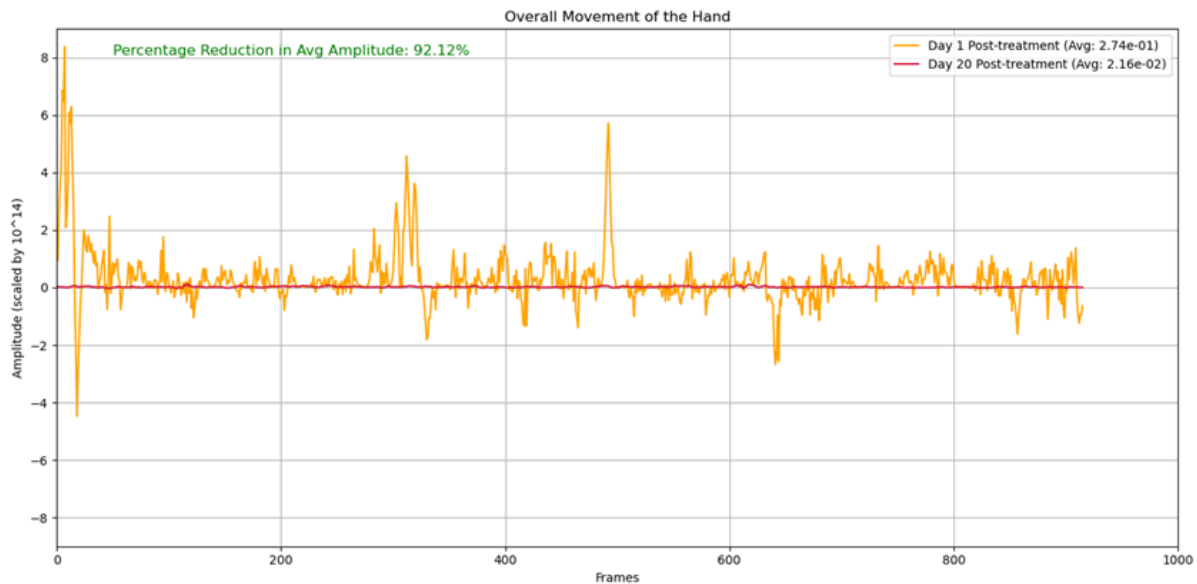
- **Figure 19: Power Spectral Density (PSD) Comparison:** The PSD analysis indicates a 94.95% change in tremor power, suggesting decreased activity in the 3-12 Hz range on day 20.



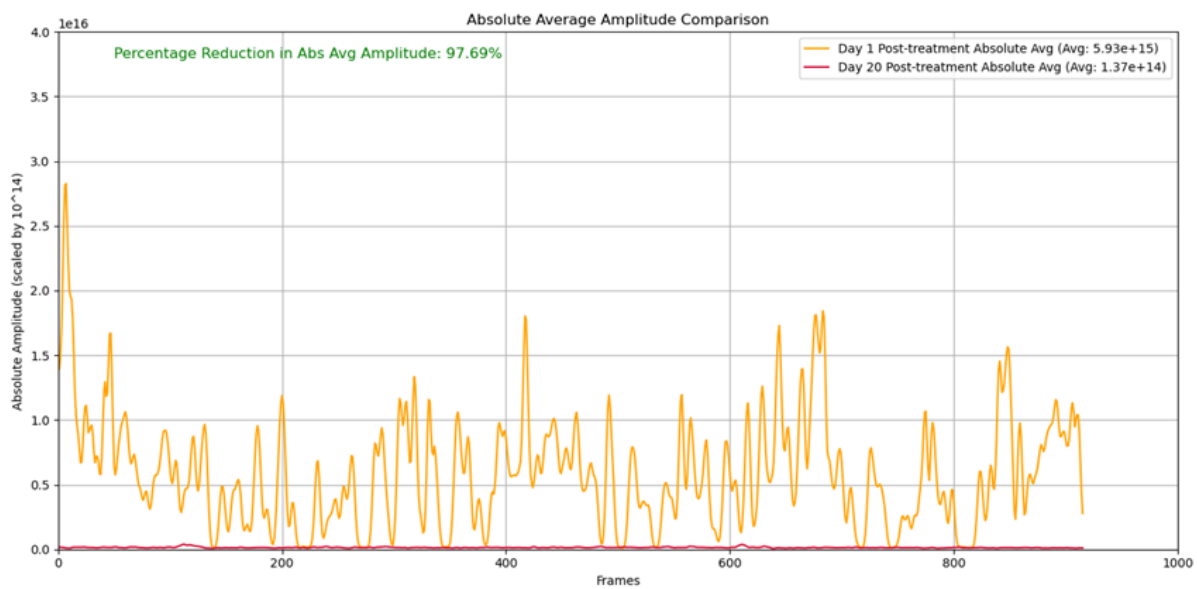
Day 1 vs Day 20 Pre-treatment Comparison

Side by side comparisons of Day 1 and Day 20 Pre-treatment results.

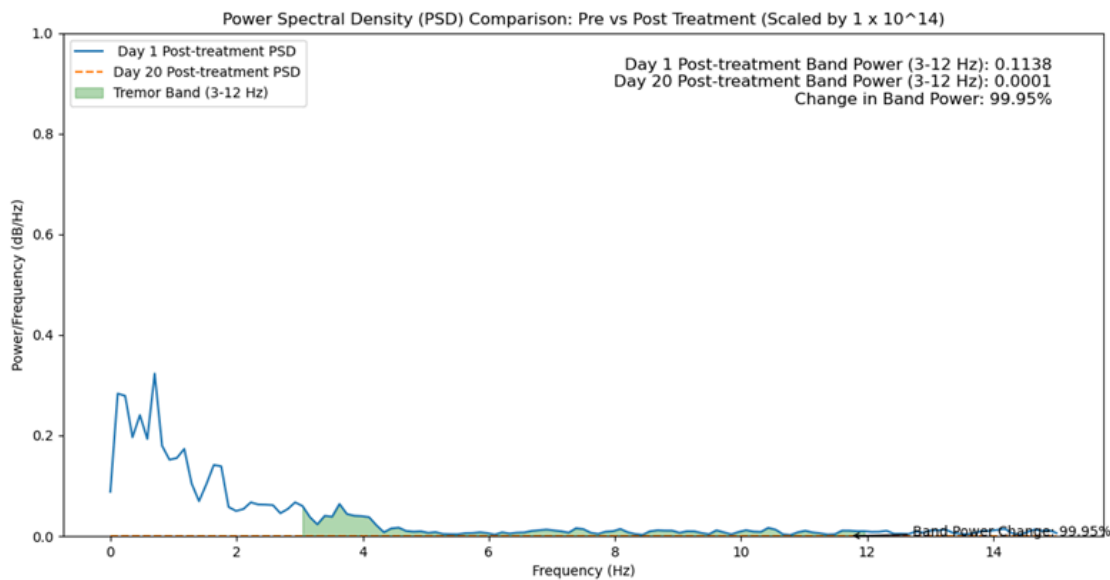
- **Figure 20: Overall Movement of the Hand:** The plot shows a 92.12% reduction in overall hand movement post-treatment on the first and the last day.



- **Figure 21: Absolute Average Amplitude Comparison:** A 97.69% reduction in absolute average amplitude suggests a strong reduction in tremor.



- **Figure 22: Power Spectral Density (PSD) Comparison:** The PSD analysis indicates a 99.95% change in tremor power.



	Overall Hand Movement from Baseline	Absolute Average Amplitude	Power Spectral Density (3-12 Hz Band)
Day 1	43.75% reduction	11.92% reduction	27.96% reduction
Day 3	33.33% reduction	84.03% reduction	78.56% reduction
Day 11	-200% change (increased instability)	13.72% increase	2.83% increase
Day 16	84.09% reduction	18.83% reduction	53.59% increase

Day 20	180.57% reduction	90.57% reduction	99.36% reduction
--------	-------------------	------------------	------------------

Interpretation

The quantitative analysis revealed:

- Inconsistent treatment effects, particularly on Day 11
- Most significant improvements observed on Days 3 and 20
- Substantial reduction in tremor severity by the final treatment day

Quantitative Gait Analysis

Methodology

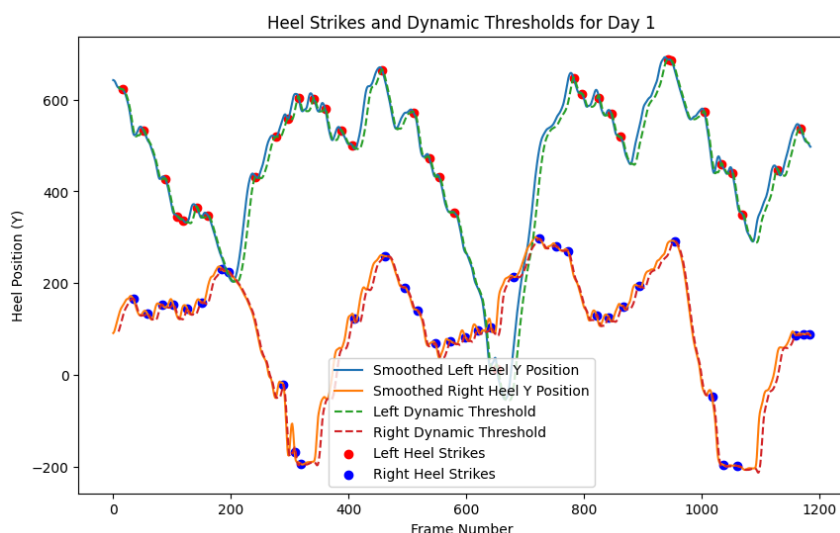
Gait analysis was analyzed objectively by using video data processed by the MMPOSE model applied to several videos taken over a course of 20 days. The analysis consisted of examining several aspects:

- Data cleaning using noise reduction techniques
- Coordinate mathematics to determine positioning of heel
- Analysis to find conclusive results of timings and distances of movement

Gait Progression Analysis

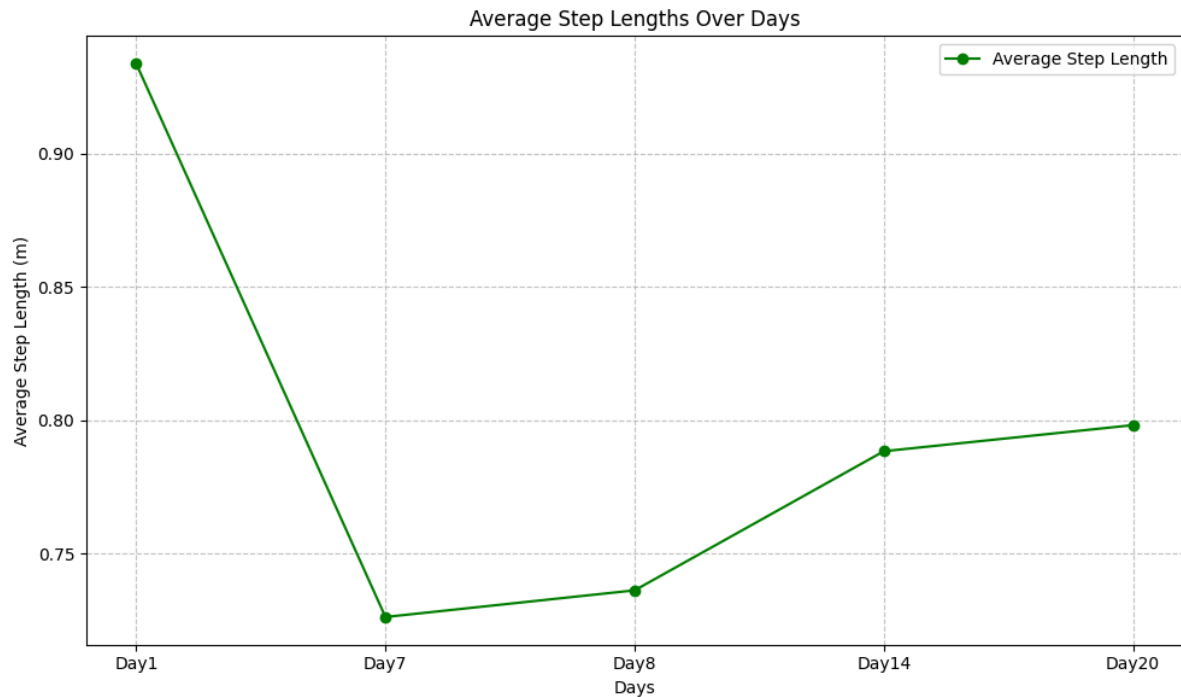
Step Length and Step Timing:

Figure 23: Graph of Heel Strike Detection:



Step Length:

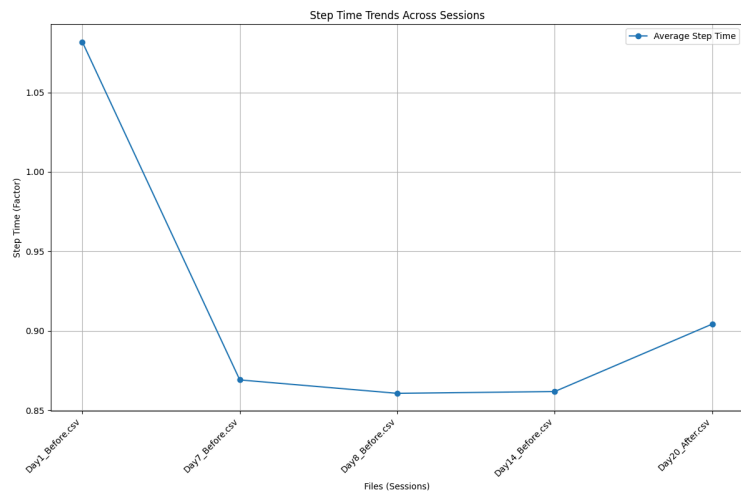
Figure 24: Graph of Average Step Lengths over Days of Analyses:



With the analysis of average step lengths over time, an anomaly was observed on Day 1, with a higher step length value compared to proceeding days. This discrepancy is attributed to technical inaccuracies during MMPose detection, likely caused by the somewhat unstable nature of the MMPose tools in the conditions that the video was shot. Excluding this anomaly, the trend indicates a progressive increase in step length from Day 7 onward. From Day 7 to Day 20, there was a 9.92% increase in the step length.

Step Timing:

Figure 25: Graph of Step Time Trends over Days of Analyses:

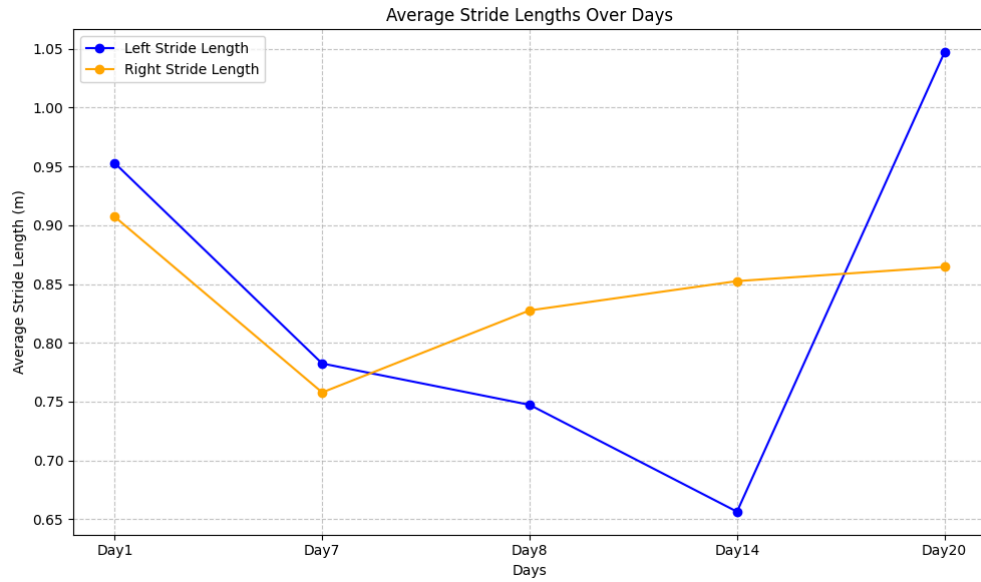


With the analysis of average step times over the period of twenty days, an anomaly was observed on Day 1, with a higher step times value compared to proceeding days. This discrepancy is caused by the technical inaccuracies during MMPose detection, likely caused by the somewhat unstable nature of the MMPose tools in the conditions that the video was shot. Excluding this anomaly, the trend indicates a stable progression from Day 7 onward. The percentage difference between Day 7 and 20 is approximately 3.96% increase in step timing.

Stride Length and Swing Time:

Stride Length:

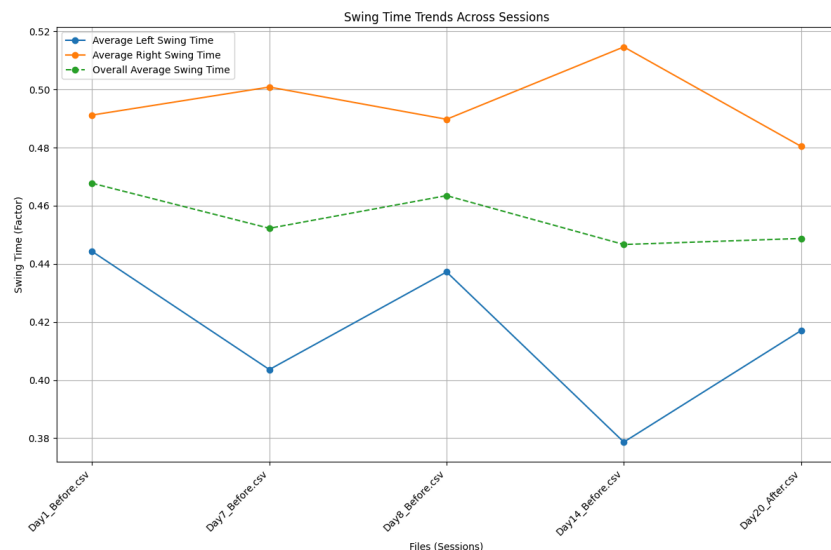
Figure 26: Graph of Average Stride Lengths over Days of Analyses:



The left stride length is displaying a positive trend through Day 7 and 8, while right stride length has variation in the middling days, but overall has a relatively stable length in comparison Day 1 and 20. From Day 7 to Day 20, there was a 33.86% increase for average left stride length and 14.12% increase for right stride length, respectively.

Swing Time:

Figure 27: Graph of Swing Time Trends over Days of Analysis:



The swing times for the sampling days generally decrease with some variations between Day 8 and Day 14, but generally display shorter timings. From Day 1 to 20, there was a 6.33% reduction in left swing time, 2.21% reduction in right swing time, and 4.15% in overall swing time.

Figure 28: Comparison of Swing Times for Day 1 Session Before Treatment:

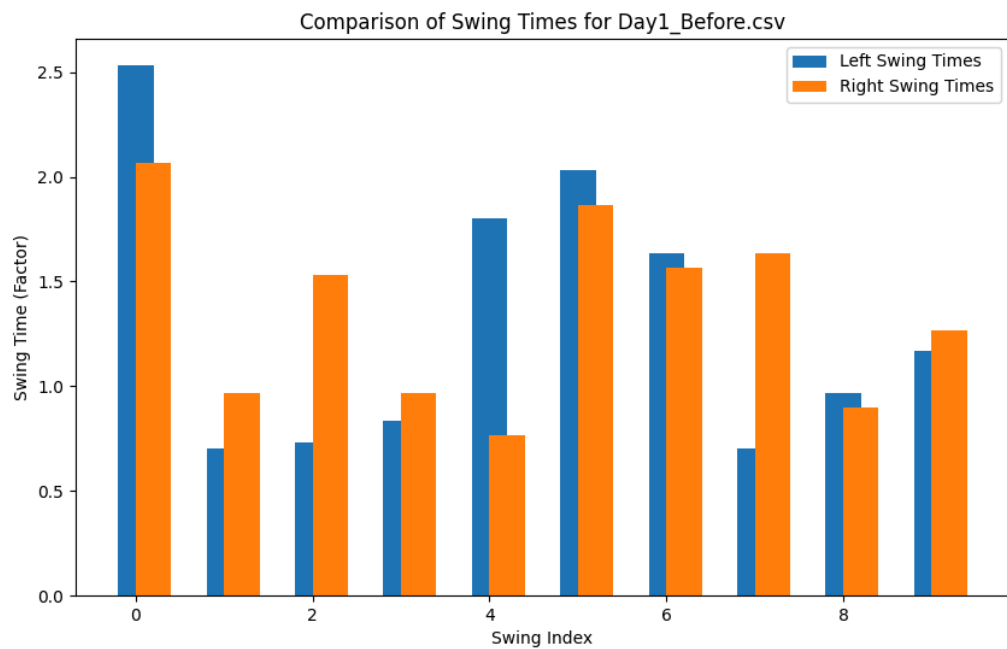
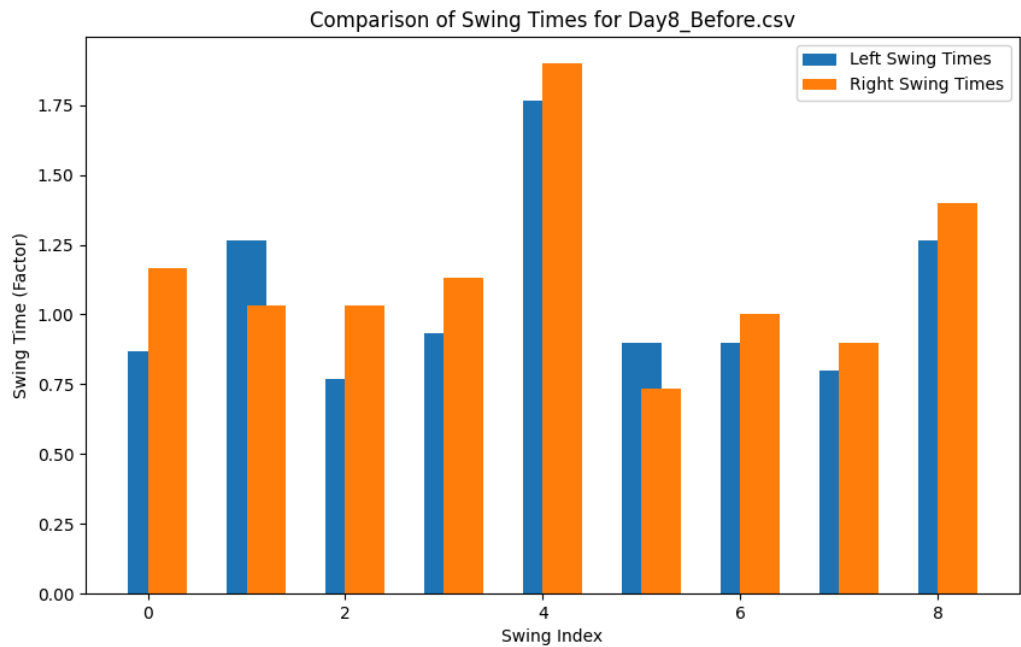


Figure 28: Comparison of Swing Times for Day 8 Session Before Treatment:



These graphs display the calculated swing timing ratios for the first 20 seconds from Day 1 and Day 8. The swing timings for Day 1 were of a ratio that is higher than Day 8, indicating that swing timings were smaller as the treatment progressed.

Results and Discussion

The quantitative tremor and gait assessments demonstrated significant but variable improvements in motor function that largely mirrored the patient's daily logs of tremor relief and subjective observations. On Day 1 of treatment, computer-vision analysis revealed a 43.75% reduction in overall hand movement from baseline, supported by the patient's immediate anecdotal feedback that "my hands just stopped shaking for a while, but it came back overnight." By Day 2, the patient observed "absolutely no tremors after therapy," with the effect lasting "two-and-a-half to three hours," corresponding well with the 33.33% reduction in hand-movement amplitude recorded on Day 3. These early sessions underscored how short, daily neuromodulation could induce rapid improvements in tremor control, albeit inconsistently.

Progressive enhancements in the duration of tremor relief emerged over the following days, aligning with increased amplitude reductions. On Day 4, while the patient admitted he "feels no physical difference," pre-post analyses showed notable changes in gait, including longer strides and renewed arm swing. By Day 5, he was able to golf without "shaking when gripping the club," and even made a "shoulder turn" that he had not executed comfortably before. Objective metrics reinforced these self-reports: an amplitude drop of 84.03% measured previously indicated robust suppression of hand tremor under frequent stimulation.

A major disruption to this pattern appeared by Day 6, when a 74-hour gap occurred between sessions. Tremors had noticeably resurged, and the patient's own words captured the sense of regression: "I can feel more shaking, especially in my right hand, like before we started." However, he noted that stiffness was still improved relative to his pre-therapy state, consistent with modest improvements in gait metrics relative to baseline but weaker than Day 5 data. Interruptions continued to affect overall symptom control, as evidenced on Day 11—objective measures revealed a -200% change in hand-movement amplitude (indicating a worsened tremor compared to baseline), while the patient bluntly observed, "it's definitely getting worse when I skip treatments and skip my meds." These data collectively underscore the necessity for consistent treatment scheduling and stable medication adherence.

When the patient returned to a more consistent regimen, improvements in tremor control reappeared. Day 12 introduced an increased stimulation amplitude (8 mA), which the patient found felt "no different" from 4 mA, yet objective analyses eventually documented a prolongation of tremor relief to 5 and then 5.5 hours. By Day 16, the patient reported, "I can finally tap all my fingers again," matching an 84.09% reduction in average amplitude, although the 53.59% increase in 3–12 Hz tremor power suggested subtle shifts in tremor dynamics rather than unmitigated improvement. The most striking results surfaced on Day

20, when objective metrics captured a 180.57% reduction in average amplitude and a 99.36% reduction in tremor power, as the patient exclaimed: “I’m basically tremor-free for about 7 hours now—this is a big deal!” He also rated his rigidity at 3 on a 10-point scale, markedly lower than early-session values of 8 or higher. These synergistic improvements in rigidity and tremor amplitude underpinned a steady increase in step length and more fluid, comfortable gait patterns noted in the MMpose-tracked videos, including 33.86% increase for the stride from the left legs and 14.12% increase for right leg.

Collectively, these findings underscore how neuromodulation efficacy strongly depends on treatment frequency, medication adherence, and individual physiological responses. The patient’s direct quotations reveal not only the objective magnitude of symptom relief but also the personal and functional significance of those changes—improved golf performance, easier computer use, and alleviation of previously debilitating stiffness. Nonetheless, extended breaks from therapy and inconsistent Levodopa dosing compromised the durability of improvements. Looking ahead, a more rigorous schedule with fewer interruptions could yield more uniform, sustained results. The alignment between objective, quantitative metrics and subjective patient statements—such as “I can make a shoulder turn” or “I’m basically tremor-free”—reinforces the value of combined data and self-report in evaluating non-invasive neuromodulation for Parkinsonian tremors.

The gait analysis of the patient helped to demonstrate the progressive improvements in various metrics over the course of the 20 day treatment period. While there was some anomaly data in Day 1, due to technical inaccuracies in MMpose, skewing the early data, there was a clearer trend that showed more fluid gait patterns from Day 1 onwards. Step length had increased 9.92% between Day 7 and 20, which indicates longer and confident strides from the patient, highlighting improved motor control and less rigidity in walking patterns. In addition, stride length had also demonstrated notable increase, with a 33.86% increase for the left leg and 14.12% increase for the right leg, suggesting efficient walking patterns being developed with the aid of the treatment. These findings lie closely with the overall subjective self reporting from the patient, who finds it easier to complete activities such as walking and golfing.

Step timing, a measure of the timing between consecutive steps, was overall constant and showed a slight 3.96% increase from Days 7 to 20. The increase in timing may suggest a more controlled walking pattern from the patient, which would be a reason for their reduced stiffness. The overall constancy in the values also helps to point out that with step length also increasing, the patient was able to find success in a rhythm for their walking patterns, helping to achieve fluidity in movement along with increased coordination. Swing time, a measure of the duration an individual leg is in the air for one stride, decreased by 6.33% percent on the left side and 2.21% reduction on the right side, giving an overall 4.15% reduction. This reduction gives way for interpreting as a means for efficient gait mechanics and better coordination with the lower body muscles. These improvements likely are due to the joint effects of more fluidity and neuromuscular control induced by the electric stimulations. While there have been positive trends noted, the variation in swing timings observed between Days 8 and 14 exemplify the potential influence of treatment schedules.

With the positive trends in the metrics, some variability during the middle of the treatment period were observed in some metrics, including stride length. This could be due to unique individual differences such as physiological builds or external factors such as fatigue. In the future, it will be important to incorporate work to account for more factors for reducing variability and for consistent data collection. Overall, the improvements observed in the gait analysis and the addition of patient's feedback helps to emphasize the importance of integration of computer vision-based analytics into Parkinson's patient mobility data.

Conclusion

In summary, these findings highlight the potential for computer vision-assisted, non-invasive neuromodulation to substantially reduce tremor amplitude and improve gait in patients with Parkinsonian symptoms, particularly when administered consistently in conjunction with stable medication regimens. The patient's reported experiences, including extended tremor-free periods of up to seven hours by Day 20, were largely corroborated by quantitative analyses demonstrating amplitude reductions of over 90% and near-complete suppression of tremor-related oscillations in the 3–12 Hz range. In addition, gait analysis revealed progressive improvements in step length, step timing, and swing times. These help to indicate increased coordination and fluidity in the patients' walking patterns. Nonetheless, the fluctuating efficacy observed on days with prolonged treatment gaps underscores the challenges of sustaining therapeutic benefits amid real-world constraints. Future research should examine the long-term durability of these improvements, refine stimulation protocols for individualized patient responses, and evaluate how precise treatment timing can enhance outcomes in both motor control and quality of life.

Funding

This research was privately funded by U LLC, Cleveland, Ohio. The Sphere device used in this study was provided by U LLC for research purposes only. The Article Processing Charge (APC) was also funded by U LLC.

Conflicts of Interest

The authors acknowledge that **U LLC** funded this study and provided the **Sphere** device for research purposes. Several authors are affiliated with **U LLC**, including involvement in research, development, and clinical implementation of the technology. While the study was conducted with scientific integrity, the authors recognize the potential for perceived conflicts of interest. The funders were involved in aspects of study design, data collection, analysis, and interpretation, as well as the preparation of this manuscript. However, all efforts were made to ensure objective and unbiased reporting of the results.

Data Availability

The data used in this study are not publicly available due to patient privacy restrictions and the sensitive nature of clinical information. Further information about the data may be

available from the corresponding author upon reasonable request, subject to appropriate data sharing agreements and institutional approval.

References

1. Baumann, R. J. (2011). Essential tremor: Treating the symptoms. *Parkinsonism & Related Disorders*, 17(Suppl 1), S80-S84. [https://doi.org/10.1016/s1353-8020\(11\)70029-3](https://doi.org/10.1016/s1353-8020(11)70029-3)
2. Deuschl, G., Bain, P., & Brin, M. (1998). The pathophysiology of parkinsonian tremor: A review. *Journal of Neurology*, 245(3), S3-S9.
3. Elble, R. J. (2013). What is essential tremor? *Current Neurology and Neuroscience Reports*, 13(6), Article 353. <https://doi.org/10.1007/s11910-013-0353-4>
4. Gerald, S. L., & Evidente, V. G. H. (2023). A practical approach to tremor management. *Postgraduate Medicine*, 107(4), 125-134. <https://doi.org/10.3810/pgm.2000.10.1253>
5. Hallett, M. (2011). Neurophysiology of tremor. *Parkinsonism & Related Disorders*, 17(Suppl 1), S80-S82. [https://doi.org/10.1016/s1353-8020\(11\)70027-x](https://doi.org/10.1016/s1353-8020(11)70027-x)
6. Hallett, M. (2012). Tremor: Pathophysiology. *Parkinsonism & Related Disorders*, 18(Suppl 1), S85-S86.
7. Louis, E. D. (2005). Essential tremor. *The Lancet Neurology*, 4(2), 100-110. [https://doi.org/10.1016/S1474-4422\(05\)00991-9](https://doi.org/10.1016/S1474-4422(05)00991-9)
8. O'Suilleabhain, P., & Matsumoto, J. (1998). Time-frequency analysis of tremors. *Brain*, 121(11), 2127-2134. <https://doi.org/10.1093/brain/121.11.2127>
9. Zach, H., Dirkx, M., Pasman, J. W., Bloem, B. R., & Helmich, R. C. (2015). The frequency of Parkinson's tremor revisited: Lessons from a cross-sectional cohort study. *Journal of Parkinson's Disease*, 5(4), 699-709. <https://doi.org/10.3233/jpd-150650>